

**DEVELOPMENT OF 3D MICROSTRUCTURES
BY USING GRAYSCALE
PHOTOLITHOGRAPHIC TECHNIQUE**

LEE TZE PIN

UNIVERSITI SAINS MALAYSIA

2016

**DEVELOPMENT OF 3D MICROSTRUCTURES BY USING
GRAYSCALE PHOTOLITHOGRAPHIC TECHNIQUE**

by

LEE TZE PIN

Thesis submitted in fulfillment of the requirements

for the degree of

Master of Science

March 2016

ACKNOWLEDGEMENTS

First and foremost, I would like to express my sincerest gratitude to my supervisor, Dr Khairudin Mohamed for his constant encouragement, valuable suggestions and guidance in making this research project successful. As a mentor, he has provided me with consistent support on the project with his knowledge and patience, while allowing me the room to work and learn on my own. I would also like to thank him for all the time spent on helping me proofread and correcting the mistakes in this thesis.

A special thank goes to the Malaysian Ministry of Higher Education for funding the tuition fees for my M.Sc. studies through the MyBrain programme. Besides, I will also take this opportunity to thank all the technical staffs at the School of Mechanical Engineering, Universiti Sains Malaysia for their invaluable technical assistance. I would also like to express my sincere thanks to all the members of Nanofabrication and Functional Materials Research Group (NFM), as they share their knowledge and advices throughout this research.

Last but not least, I would like to thank my loving parents for their continuous support and encouragements throughout my M.Sc. studies at USM. For those who have directly and indirectly contributed to the accomplishment of this thesis, thank you very much.

TABLE OF CONTENTS

Acknowledgements	ii
Table of Contents	iii
List of Tables.....	vii
List of Figures	viii
List of Abbreviations.....	xv
List of Symbols	xvii
Abstrak	xviii
Abstract	xx

CHAPTER 1: INTRODUCTION

1.1 3D Microfabrication.....	1
1.2 Lithography	2
1.2.1 Photolithography	3
1.2.2 Extreme Ultraviolet Lithography (EUVL).....	5
1.2.3 Electron Beam Lithography (EBL).....	7
1.2.4 Focused Ion Beam Lithography (FIB)	9
1.3 Problem Statement	11
1.4 Research Objectives	12
1.5 Scope of Research.....	12
1.6 Thesis Outline	13

CHAPTER 2: LITERATURE REVIEW

2.1	Overview of 3D Photolithography	14
2.1.1	Variants of 3D Photolithography	14
2.1.2	Multiple-Step Photolithography	14
2.1.3	Direct-Write Photolithography	17
2.1.4	Grayscale Photolithography	19
2.2	Classification of Grayscale Photomask.....	20
2.2.1	Chrome Halftone Grayscale Photomask	22
2.2.2	LDW Glass and HEBS Glass Grayscale Photomask	24
2.2.3	Bimetallic Grayscale Photomasks.....	26
2.3	Literature Findings	29
2.4	Grayscale Photolithography Process.....	31
2.4.1	Surface Preparation	31
2.4.2	Photoresist Spin Coating.....	33
2.4.3	Soft Baking	36
2.4.4	UV Exposure.....	37
2.4.5	Post Exposure Baking	40
2.4.6	Developing	41
2.4.7	Hard Baking	42
2.5	Summary of Photolithographic Process	43

CHAPTER 3: METHODOLOGY

3.1	Overview of The Procedures.....	44
3.2	Design of Grayscale Photomask	45
3.3	Master Mask Film Printing	48
3.4	Fabrication of Emulsion Mask.....	52
3.4.1	Emulsion Mask Exposure	52
3.4.2	Emulsion Mask Development.....	54
3.5	Fabrication Of 3D Microstructure.....	56
3.5.1	Sample Preparation	56
3.5.2	Photoresist Coating	58
3.5.3	Soft Baking	59
3.5.4	UV Exposure.....	62
3.5.5	Post Exposure Baking	64
3.5.6	Develop	65
3.5.7	Hard Baking	66
3.6	Adhesion Issue	66
3.7	Evaluation of Photoresist Thickness	66
3.8	Demonstration of 3D Microfabrication.....	68

CHAPTER 4: RESULTS AND DISCUSSION

4.1	Overview	70
-----	----------------	----

4.2	Adhesion Issue	70
4.2.1	Soft Baking Parameter	71
4.2.2	Cooling Time of Post Exposure Baking	76
4.3	Evaluation of Photoresist Thickness	80
4.3.1	Results of 10 % Interval Grayscale Concentration	80
4.3.2	Results of 2 % Interval Grayscale Concentration	82
4.4	3D Microfabrication Demonstration	85
4.4.1	Microfluidic Channel	85
4.4.2	Curvature structure (Concave and convex shape).....	93

CHAPTER 5: CONCLUSION AND RECOMMENDATIONS

5.1	Conclusion	100
5.2	Recommendations	102

References	103
------------------	-----

List of Publications

LIST OF TABLES

		Page
Table 2.1	The capability of each 3D microfabrication method for comparison.	30
Table 3.1	Master mask film printed results obtained by several tested printers.	50
Table 4.1	Rating scale of photoresist stickiness.	72
Table 4.2	The effects of soft baking time at temperature of 120 °C to the result of developed sample.	72
Table 4.3	The effects of soft baking time at temperature of 95 °C to the result of developed sample.	73
Table 4.4	Effect of cooling time of post exposure bake to the adhesion result of developed sample.	77
Table 4.5	Result of the developed photoresist thickness obtained by using 30 s and 60 s of UV exposure time.	83
Table 4.6	Selection of the grayscale concentration in the fabrication of microfluidic device.	87
Table 4.7	Thickness of the developed photoresist at each different grayscale concentration.	88
Table 4.8	Surface topology of the developed photoresist at each different grayscale concentration	89

LIST OF FIGURES

		Page
Figure 1.1	SEM image of a microchannel surface with 3D micro-square elements [1].	2
Figure 1.2	Basic steps of photolithographic process include (a) photoresist spin coating, (b) UV light exposure and (c) pattern development where (d) is the final result of photolithographic process [6].	4
Figure 1.3	Schematic of EUVL optical system [13].	6
Figure 1.4	The schematic diagram of the electron beam lithography system [22].	8
Figure 1.5	The schematic diagram of the focus ion beam lithography system [29].	10
Figure 2.1	SEM image of “woodpile” photonic-crystal structures with a) 3 stacked photoresist layers and (b) four stacked photoresist layers fabricated by using multi-layer photolithography [31].	15
Figure 2.2	SEM image of 1 mm diameter gear together with 4 of its alignment marks formed by multiple-layer (5 layers) lithography [32].	16
Figure 2.3	Bottom up exposure method. (a) Schematic of how multi-layer structures are generated. (b) Scanning electron micrograph of two-layer SU-8 pillars, and (c) Higher magnification micrograph at the base of the two-layer pillars [33].	16
Figure 2.4	Schematic of direct writing process [34].	17

Figure 2.5	SEM image of a linear concave lens structure fabricate by exposing electron beam with 0.5-mm pixel size on SU-8 photoresist [36].	18
Figure 2.6	Photoresist pyramid fabricated by using Heidelberg DWL66FS Laser Pattern Generator [37].	18
Figure 2.7	Schematic of the lithographic process in case of (a) conventional lithography and (b) grayscale lithography.	20
Figure 2.8	Grayscale pattern of (a) a halftone pattern and (b) an analogue pattern, (c) and (d) are the enlarged images of the framed picture in (a) and (b), respectively [42].	21
Figure 2.9	Image of (a) halftone generated by using pulse-width modulation and (b) is the grayscale image equivalent to the halftone [41].	22
Figure 2.10	Principle of halftone coding (a) pulse-width modulation (PWM) where the size of dots change for each grayscale level; (b) pulse-density modulation (PDM) where the pitch of dots change; (c) combination of both PWM and PDM where the size and pitch of the dots change; (d) the resulting grayscale [41]	23
Figure 2.11	Image of photoresist wedge structure fabricated by using PWM halftone photomask. The wedge is 69 μm long and 5 μm tall [45].	24
Figure 2.12	SEM images of Fresnel lenses in AZ 5214 photoresist [49].	26

Figure 2.13	Process of fabricating bimetallic grayscale photomask. (a) Bi/In or Sn/In are sputtered on glass or quartz substrate; (b) Bi/In or Sn/In form into a new transparent alloy when exposed to laser beam, the unexposed area remains to be opaque metal structure; (c) bimetallic layers are used as single exposure grayscale mask [40].	27
Figure 2.14	SEM image of 3D structures created in SU-8 using the backside exposure method [42].	28
Figure 2.15	Examples of contact angles of water droplets on (a) hydrophilic surface, CA 20°; (b) optimum for resist adhesion, CA 70°; (c) hydrophobic surface, CA 95° [2].	33
Figure 2.16	Photoresist spin coating process. (a) A controlled amount of photoresist is dispensed by using dropper. (b) The dispensed photoresist is allowed to spread across the wafer. (c) The turntable is spin in low rpm to allow the photoresist to eliminate excess photoresist. (c) The turntable is rapidly ramped-up to high rpm so that a thin and uniform layer of photoresist is formed [54].	34
Figure 2.17	Photoresist spins speed curves for different resist viscosities [2].	35
Figure 2.18	Reaction of polymer during exposure process. (a) Polymer chain scission on positive resist. (b) Polymer cross-linking on negative resist [5].	36
Figure 2.19	Different types of exposure system (a) contact lithography (b) proximity lithography and (c) projection lithography [3].	39
Figure 2.20	Schematic of the lithographic process in case of (a) top exposure and (b) back exposure [39].	40

Figure 2.21	Image of standing waves effect on the sidewalls of resist feature [2].	41
Figure 2.22	Schematic of selective developing process of (a) negative photoresist and (b) positive photoresist [3].	42
Figure 3.1	Overall methodology flow chart used in the present study.	44
Figure 3.2	Examples of photomask polarities: (a) Clear field photomask (b) Dark field photomask [4].	46
Figure 3.3	Process of determining the polarity of software-drawn mask.	47
Figure 3.4	Design of grayscale mask with 10 different grayscale concentration levels.	48
Figure 3.5	Image of designed micro-rectangles with height of 400 μm and length of 50 μm .	49
Figure 3.6	Optical image of printed micro-rectangles by using a USB Digital Microscope with 800x magnification.	51
Figure 3.7	Image of a blank unexposed silver halide coated emulsion mask.	52
Figure 3.8	Printed master mask film was placed at the centre of the light box.	53
Figure 3.9	Pattern from master mask film projected 5 times smaller and inverted on frosted glass.	54
Figure 3.10	Image of dark field emulsion mask after development process.	55
Figure 3.11	Flow chart for fabrication of 3D microstructure.	56
Figure 3.12	Figure 3.12 Image of water droplet formed before and after the surface cleaning process where (a) shows hydrophilic surface and (b) shows hydrophobic surface.	57

Figure 3.13	Glass substrate coated with thick SU-8 2010 photoresist.	58
Figure 3.14	Image of the deformed photoresist with non-uniform coating surface.	60
Figure 3.15	Image of under baked photoresist with low viscosity.	61
Figure 3.16	Image of normal soft baked photoresist with high viscosity.	61
Figure 3.17	Image of (a) over-baked yellowish colour photoresist and (b) transparent photoresist after suitable soft bake time.	62
Figure 3.18	Manually aligned SU-8 coated glass samples on top of grayscale emulsion mask.	63
Figure 3.19	Equipment setup for UV exposure.	63
Figure 3.20	Visible latent image of emulsion mask pattern in SU-8 photoresist coating.	64
Figure 3.21	IPA solution turns cloudy white on the surface of exposed pattern.	65
Figure 3.22	Schematic diagram of the CMM measurement setup.	67
Figure 3.23	Design of 2 % grayscale interval mask from the range of 50 % grayscale concentration to 100 % grayscale concentration. a) Software designed mask. b) Dark field emulsion mask.	68
Figure 3.24	Schematic diagram of the optical measurement setup.	69
Figure 4.1	Image of peeled off SU-8 photoresist layer after development process.	70

Figure 4.2	The effect of excessive solvent contain to the mechanical stability of microstructure. (a) Excessive solvent contain will lead to low mechanical stability. (b) Sufficient solvent contain will result in high mechanical stability.	75
Figure 4.3	Formation of tensile and compressive stress in the coated photoresist layer and the glass substrate during polymerization shrinkage.	76
Figure 4.4	Graph of temperature changes of each sample during the cooling period.	78
Figure 4.5	Images of developed photoresist layer after it was left to cool for a) 0 min, b) 15 min, c) 30 min, d) 45 min and 60 min after post exposure baking process.	79
Figure 4.6	Image of a bowing photoresist.	80
Figure 4.7	Effect of grayscale concentration to the developed photoresist thickness.	81
Figure 4.8	Graph of percentage of grayscale concentration versus the thickness of developed photoresist.	84
Figure 4.9	CorelDraw designed grayscale mask of the simple microfluidic channel.	86
Figure 4.10	Cross section (a-b) of the microfluidic channel at Section D.	86
Figure 4.11	Image of (a) grayscale emulsion mask of the simple microfluidic channel and (b) SU-8 photoresist microfluidic channel.	87
Figure 4.12	The design of 2 parts of grayscale mask. (a) Grayscale design of the microfluidic without micro-pores. b) Binary mask of the micro-pores.	90

Figure 4.13	Image of the developed SU8- photoresist after the first cycle of grayscale photolithography process.	91
Figure 4.14	Image of developed glass sample coated with second layer of SU-8 photoresist.	92
Figure 4.15	Image of microfluidic channel completed with micropores in the microchannel.	92
Figure 4.16	Fabrication of curvature structure along microfluidic channel. (a) Master mould fabrication (b) PDMS casting and (c) replication of PDMS curvature structure.	93
Figure 4.17	The designed grayscale mask of the microchannels. (a) Convex microchannel and (b) concave microchannel.	94
Figure 4.18	Image of the fabricated master mould of both different designs of microchannels. (a) Convex microchannel and (b) concave microchannel.	95
Figure 4.19	SEM image of the fabricated of 3D microchannel on a master mould made of developed SU-8 photoresist. (a) Convex microchannel and (b) concave microchannel.	96
Figure 4.20	Cross section profile of microchannel on master mould. (a) Convex microchannel and (b) concave microchannel.	97
Figure 4.21	Image of PDMS microchannel. (a) Concave PDMS microchannel (b) convex PDMS microchannel.	98
Figure 4.22	Cross section profile of microchannel on PDMS. (a) Concave microchannel and (b) convex microchannel.	99

LIST OF ABBREVIATIONS

2D	2-dimensional
3D	3-dimensional
Bi	Bismuth
CAs	Contact angles
CoG	Chrome-on-glass
DI	Deionised
dpi	Dot per inch
EBL	Electron beam lithography
EUVL	Extreme ultraviolet lithography
FIB	Focused ion beam lithography
H ₂ O ₂	Hydrogen peroxide
HCl	Hydrochloric acid
HEBS	High Energy Beam Sensitive
HF	Hydrofluoric
IC	Integrated circuit
In	Indium
IPA	Isopropyl alcohol
LDW	Laser Direct Write
MEMS	Micro-electromechanical-systems
Mo	Molybdenum
NFM	Nanofabrication and Functional Materials
NGL	Next Generation Lithography
NH ₃	Ammonia

PDM	Pulse-density modulation
PDMS	Poly-dimethyl-siloxane
PET	Polyethylene terephthalate
PMMA	Polymethyl methacrylate
PWM	Pulse-width modulation
rpm	Revolution per minute
SEM	Scanning electron microscope
Si	Silicon
Si-OH	Silanol groups
Sn	Tin
UV	Ultraviolet light

LIST OF SYMBOLS

CD	Minimum feature size
λ	Wavelength of light source
NA	Numerical aperture
θ	Contact angle
UV_{dosage}	UV exposure dosage
$UV_{\text{intensity}}$	UV illumination intensity
t_{exposure}	UV exposure time

PEMBANGUNAN MIKROSTRUKTUR 3D MENGGUNAKAN TEKNIK FOTOLITOGRAFI SKALA KELABU

ABSTRAK

Perkembangan pesat teknologi seperti bio-chip, peranti pendalir mikro, peranti mikro-optik dan sistem mikro elektro-mekanikal (MEMS) memerlukan keupayaan membina struktur tiga dimensi (3D) yang kompleks di skala mikro. Bagi membina struktur 3D di skala mikro, kebiasaannya beberapa topeng cahaya digunakan bagi menghasilkan corak 3D diatas beberapa lapisan photoresist yang ditindan. Namun begitu teknik ini memakan masa, tidak efisien dan rumit untuk diadaptasi dalam industri pembuatan. Teknik lithografi terbaru seperti litografi menggunakan pancaran elektron (EBL), pancaran ion terfokus (FIB) dan sinar ultraviolet ekstrem (EUV) memerlukan kos terlalu tinggi dan kepakaran yang mahir dalam bidang tersebut. Tujuan utama kajian ini adalah untuk menghasilkan teknik mudah bagi menghasilkan struktur 3D pada skala mikro menggunakan topeng emulsi dengan teknik litografi skala kelabu. Kajian dimulakan dengan mencari prosedur dan parameter yang sesuai bagi menghasilkan hasil microfabrikasi yang optimum. Dalam eksperimen ini, kepekatan skala kelabu ditentukan dengan mengawal peratusan titik hitam di sesuatu kawasan. Peratusan skala kelabu yang tinggi akan menghasilkan struktur mikro yang lebih tebal. Corak yang telah direka akan dicetak di atas kertas plastik lutsinar. Corak ini yang akan dipindahkan ke atas topeng kaca emulsi (Plat Cahaya Berprestasi Tinggi). Plat ini dihasilkan oleh Konica Minolta Inc. Selepas itu, corak dari topeng kaca emulsi akan dipindahkan ke atas photoresist MicroChem SU-8 2010 yang telah didepositkan di atas substrak kaca. Dengan menggunakan teknik mikrofabrikasi ini, struktur mikro antara 17 μm sehingga 750

μm dapat dihasilkan dengan hanya menggunakan sekali pendedahan cahaya sahaja. Kajian seterusnya adalah untuk menghasilkan saluran mikrofluidik menggunakan teknik litografi skala kelabu. Saluran mikrofluidik ini dinilai menggunakan sistem mengukur Infinite Fokus daripada ALICONA dan mikroskop imbasan elektron (SEM). Dengan menggunakan teknik mikrofabrikasi ini, liang yang berdiameter 35 μm telah berjaya dihasilkan dalam saluran mikrofluidik. Kesimpulannya, ketebalan struktur mikro adalah ditentukan oleh peratusan skala kelabu di peringkat mereka bentuk.

DEVELOPMENT OF 3D MICROSTRUCTURES BY USING GRAYSCALE PHOTOLITHOGRAPHIC TECHNIQUE

ABSTRACT

Recently, the rapid development of technology, such as biochips, microfluidic device, micro-optical devices, and micro-electromechanical-systems (MEMS), demands the capability to create complex designs of three-dimensional (3D) microstructures. Nevertheless, in order to create 3D microstructures, the traditional photolithography process often requires multiple photomasks to generate a 3D pattern from several stacked photoresist layers. This fabrication method is extremely time consuming, has low throughput, and is complicated for high volume manufacturing scale. On the other hand, the next generation lithography, such as electron beam lithography (EBL), focused ion beam lithography (FIB), and extreme ultraviolet lithography (EUV) is however too costly and requires experts to setup the machines. Therefore, the purpose of this study had been to develop a microfabrication method in producing 3D curvature microstructures by employing the single-step grayscale emulsion mask photolithography technique. In the first part of this study, suitable procedure and parameters were determined to produce optimum microfabrication results. In the experiment, the concentration of grayscale was determined by the percentages of halftone dots filling in a particular area. Therefore, the lower the concentration of halftone dots on the emulsion mask, the thicker the developed microstructure will be. First, the designed patterns were printed out on a transparent sheet. Then, the patterns were transferred onto an emulsion glass mask (High Precision Photo Plate) from Konica Minolta, Inc. After that, SU-8 2010 negative photoresist (MicroChem) was deposited on a glass substrate, while the

patterns from the emulsion glass were transferred onto a photoresist coated glass substrate. From this microfabrication method, a microstructure with maximum and minimum thickness of 750 μm and 17 μm respectively had been obtained in a single-step lithography exposure. On the other hand, as for the second part of this study, this grayscale fabrication method was demonstrated on the fabrication of microfluidic channel. The microfluidic channel was then evaluated under InfiniteFocus measurement systems from ALICONA and also under scanning electron microscope (SEM). By using this microfabrication method, microfluidic channel with 35 μm pores was successfully fabricated. Therefore, it is concluded that different thickness of developed photoresist can be obtained by manipulating the percentage of grayscale concentration during the mask designing stage.

CHAPTER 1

INTRODUCTION

1.1 3D MICROFABRICATION

The rapid growth of technology has increased the efficiency and the quality of our lives. Therefore, in order to cope with the pace of technology development, micro and nanofabrication skills have been increasing in demand over each year. These days, technologies such as biochips, microfluidic device, micro-optical devices, and micro-electromechanical-systems (MEMS), are designed in more complex three-dimensional (3D) micro-profiles. In fact, some of the benefits of designing 3D microstructures are to maximize the functional efficiency, as well as to minimize the space and material consumption.

For example, in a microfluidic device, the geometry of microchannel in a micromixer plays an important role during the fluidic mixing process. However, a straight microchannel could only produce laminar flow, which is less favourable for the mixing process. Hence, 3D microfabrication is important to improve the properties of fluidic handling by creating well-defined 3D microstructures in the microchannel. Figure 1.1 illustrates an image taken by using scanning electron microscope (SEM) where the 3D microstructures were fabricated inside the microchannel in order to increase the surface roughness in the microchannel, as well as to generate a turbulent flow that could ease the mixing process [1].

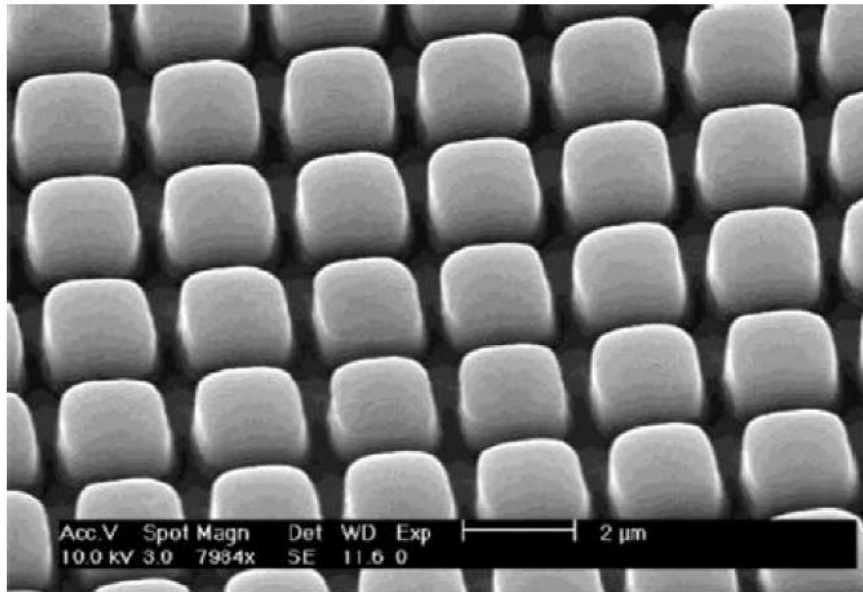


Figure 1.1 SEM image of a microchannel surface with 3D micro-square elements [1].

1.2 LITHOGRAPHY

The key for microfabrication process is the patterning process where it determines the feature size of the microstructures. Among all patterning techniques, lithography is the most commonly used method especially in the fabrication of integrated circuit (IC) [2]. The word ‘lithography’ comes from Greek; ‘lithos’ means stones, while ‘graphia’ means write [3]. As suggested by the name, lithography literally means writing on stones. In most cases of microfabrication, stones are referred as substrates and the patterns are written on substrates by using a light sensitive polymer called photoresist.

Recently, many different forms of lithography technique have been employed by the industry. The most common form of lithography used is the photolithography technique. In the IC industry, patterns are transferred from photomask onto substrate via photolithography [4]. However, due to the endless demand of critical feature size